Proceedings World Geothermal Congress 2010
Bali, Indonesia, 25-29 April 2010

Interpretation of the Tracer Test of Balçova Geothermal Field

Serhat Akın[1], Mahmut Parlaktuna[1], Tolga Sayık[2], Hasan Sezer[2], Cetin Karahan[3] and Safa Bakrac[3]

[1]Middle East Technical University, Petroleum and Natural Gas Engineering, 06531 Ankara – Turkey

[2]İzmir Geothermal Energy Co., Balçova – İzmir

[3]General Directorate of Mineral Research & Exploration, Izmir

serhat@metu.edu.tr, mahmut@metu.edu.tr, tolgasayik@izmirjeotermal.com, hasansezer@izmirjeotermal.com

Keywords: Balcova, Rhodamine B, NaCl, tracer, mathematical model

ABSTRACT

A successful two well tracer test was conducted in Balcova - Narlidere Geothermal field (Turkey) where Rhodamine B and NaCl salt were injected from two separate injection wells. Observation of Rhodamine B and increase in the NaCl concentration in all production wells indicated that the production and injection wells are connected along the Agamemnon fault. Analysis of mean arrival time arrow plots showed the presence of several orthogonal fracture systems. Mathematical modeling results showed that NaCl tracer profiles were modeled by double porosity models. On the other hand, Rhodamine B tracer return curves were matched with fracture-matrix and multifracture models. It was found that as the production well depth becomes deeper the number of interstitial velocity inflection points increases showing that the well produces from more than one fracture systems.

1. INTRODUCTION

Izmir (Turkey) has a total of 11 important geothermal areas: Seferihisar (Karakoç, Doğanbey, Cumalı and Tuzla), Balçova-Narlıdere, Dikili (Kaynarca, Bademli, Çamur, Nebiler, Kocaoba), Bergama (Güzellik, Dübek, Paşa), Çeşme (Ilıca, Alaçatı, Şifne), Aliağa (Ilıcaburnu, Samurlu, Güzelhisar, Biçer, Helvacı), Çiğli-Menemen (Ulukent), Urla (Gülbahçe), Bayındır (Vardar), Menderes and Kemalpaşa. Among these fields, Balçova – Narlıdere geothermal (BNG) field is located only a few km to downtown Izmir near the Aegean shores. Early resistivity, self-potential (SP) and gravity surveys (Tezcan, 1962 and Ercan et al., 1986) identified a NE-SW striking fault (that is later named as Agamemnon fault) and indicated the presence of hot water under the bed of the Ilica Stream. The deep and shallow wells of BNG field produces from Izmir flysch (~300 to 1100 m depth) that is composed of lightly metamorphosed sandstones, clays and siltstones and alluvium (shallow ~ up to 100 m depth) respectively. Agamemnon fault and its associated fracture systems allow thermal waters flow into the alluvium and permeable flysch. Being one of the world's largest district heating systems Balcova district heating project has started in 1996. By the end of 2008 more than 2,450,000 m^2 comprising apartment buildings, two hotels, several public and private sector buildings, university buildings including a hospital and 6 greenhouses are now heated by geothermal energy. A total of 13 deep and 31 shallow wells have been drilled since 1963. Currently, BNG field has 11 active production and 4 injection wells (Figure 1 and Table 1). The details of early field operations are reported in Aksoy et al (2008).

Table 1. Production and Injection Well Properties.

Well	Year	Depth (m)	Pump Depth (m)	T (°C)	Flow Rate (m^3/hr)
B-5	1983	125	72	102.0	140
B-10	1989	125	48	97.0	200
BD-1	1994	564	90	110.0	60
BD-2	1995	677	90	132.0	180
BD-4	1998	624	100	135.0	180
BD-5	1999	1100	150	115.0	80
BD-6	1999	606	150	135.0	120
BD-7	1999	700	150	115.0	80
BD-9	2003	772	100	138.5	360
BD-11	2007	716	105	140.0	360
BD-14	2007	125	371	125.0	140
BD-3	1993	750	REINJECTION WELLS		
BD-8	1999	630			
BD-10	2004	750			
BD-15	2007	472			

A lumped parameter modeling study carried out by Satman et al (2002) suggested that the natural fluid recharge was about 50 kg/s and the total heat input to the system was in the between 24 and 33 MW_t range. Shallow re-injection (depth < 160 m) was preferred during the early days of the field. A total of 5 tracer tests were conducted in early 2000's to evaluate and compare the performances of shallow and deep re-injection of waste water. Three tests were conducted by using a shallow well (B-9) for re-injection while deep production wells were closed. Since small amounts (approximately 1 kg) of tracer (Uranine) were injected from B-9 in first two of the shallow tracer tests while keeping the deep production wells closed tracer was not detected in the produced waters. The analysis of the last test, on the other hand, showed that tracer velocity changed between 2.6 m/hr to 12.7 m/hr with a dispersivity of 0.01 m^2/hr. During these tests several degrees of temperature drops were observed in B-4 and B-10 wells. Tracer tests conducted in deeper BD-2 well were not successful because only 0.95 and 3 kg of Uranine were injected as a slug. It was reported that tracer return curves were not analyzable but Uranine was observed in all wells (Aksoy, 2001). Shallow reinjection practice was switched to deeper reinjection after 2002. Since then several alternative re-injection locations have been practiced to optimize re-injection and thus waste water disposal problem.

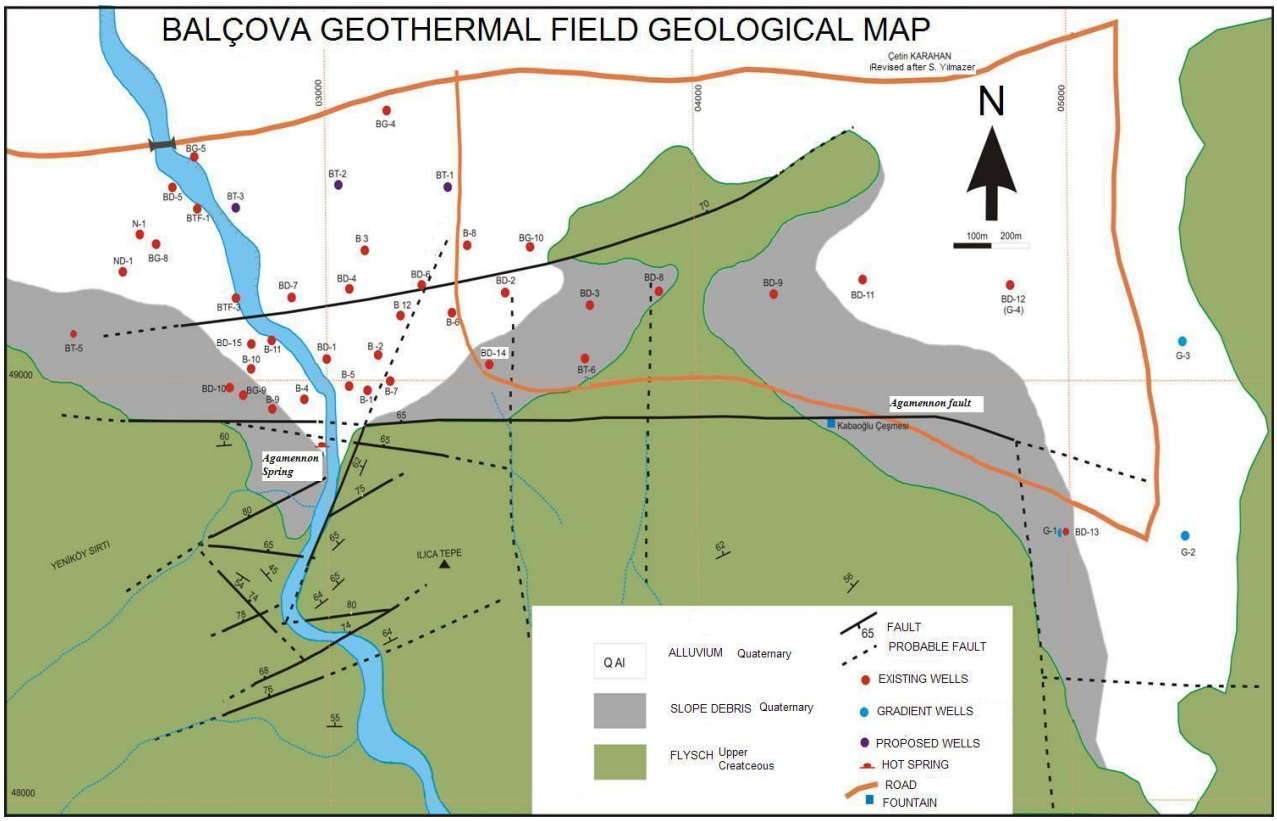

Figure 1: Location of production and injection wells in Balçova-Narlıdere Geothermal field

This paper reports the results of a long term dual tracer test conducted in BNG field using Rhodamine and NaCl salt during November 2008 and March 2009. First, tracer test design carried out using EHDT method (Field, 2003) will be introduced. After reporting tracer test implementation and measurement techniques, tracer test analysis methodologies where moment analysis introduced by Shook (2005) and tracer concentration matches to several mathematical models (Akin, 2001) will be discussed using tracer return curves.

2. TRACER TEST DESIGN

In order to evaluate the performance of the re-injection operation carried out using two injection wells a tracer test, which is the most common method of monitoring fluid communication between the re-injection sites and productions areas, was designed. In order to achieve this goal, two different tracers (Rhodamine B dye and NaCl salt) were selected based on availability, ease of use and environmental concerns. Rhodamine B was selected due to its thermal stability at reservoir conditions (140°C) and its low detection limit with a fluorimeter. NaCl salt on the other hand occurs naturally in BNG reservoir. In order to determine the amounts of Rhodamine B and salt to be mixed in the geothermal fluids and the sampling frequencies in re-injection wells EHTD method introduced by Field (2003) was used. This method depends on the solution of Equation 1.

$$R_d \frac{\partial C}{\partial t} = D_z \frac{\partial^2 C}{\partial z^2} - \upsilon \frac{\partial C}{\partial z} - \mu z \qquad (1)$$

Where R_d is dimensionless dissolving factor, C is concentration, t is time, D_z is axial diffusion constant, υ is the average velocity, μ is viscosity. In this equation, the assumptions are such that the tracer is injected as a slug and that no reaction takes place between the fluids and the formation.

$$f(x^*) = C_p - \frac{M}{An_e\sqrt{4\pi D_z t_p}} \qquad (2)$$

In order to use Equation 2 the mass of the tracer chemical, M, flow rate Q, porosity, n_e, axial dispersivity D_z, area A and the peek concentration time, t_p, should be known. Field used the functional dependence of these parameters on flow rate and travel time in order to determine the tracer concentration, tracer mass and axial dispersivity by using the tank reactor assumption where mixing occurs continuously. For the unknown parameters, correlations were used.

Using the EHTD method and assuming that *Rhodamine B* will be injected from re-injection well (BD – 8) with a flow rate of 1160 m^3/hr, for a 250 m thickness reservoir formation with 1.0% porosity for a well separation of 1335 m (i.e. distance between BD-8 and BD-5), 74.4 kg tracer chemical must be injected in order to obtain 10 µg L^{-1} of tracer at mean arrival time. It was assumed that the tracer will be injected as a slug. The expected values of chemical concentration and sampling times (open circles) are shown in Figure 2. A sensitivity study was conducted to evaluate the effect of differing re-injection rates and it was found that the amount of tracer changes exponentially from 51.4 kg to 176 kg as the rate decreased from 2160 to 560 m^3/hr (Figure 3). Porosity sensitivity runs indicated that 1% porosity increase resulted in approximately 13% increase in tracer mass. The flow rate measurements carried out in 2007 – 2008 season indicated that injection rate changed between 400 m^3/hr and 900 m^3/hr. Expecting a similar behavior 100 kg of Rhodamine B amount was selected for the test. The actual injection rate change during the test is given in Figure 4. The integral averaged injection rates of BD-8 and BD-10 are 628.57 m^3/hr and 67.9 m^3/hr, respectively. A similar

approach was followed for the amount of BD-10 NaCl tracer determination. In order to achieve this goal, first background salt concentration of the produced geothermal fluid in each production well is determined. It was observed each well showed a unique background NaCl concentration that varied between lower 200 ppms to higher 300 ppms. Following Horne (1987) 1 tonnes of NaCl has been added to the re-injected waste water in order to create a significantly higher concentration (by a factor of 3) than the background concentration and the lower detection limit of the chlorine electrode (reproducibility ±2%) that was used to measure the chlorine concentration.

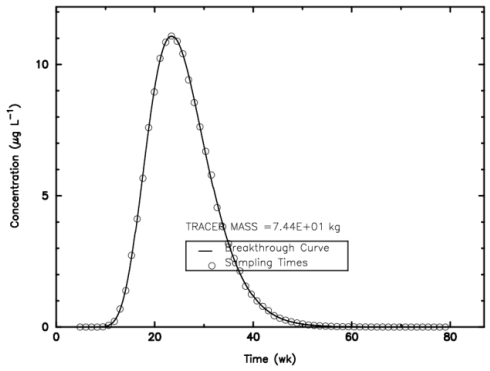

Figure 2: Expected tracer concentration – time plot showing sampling times (open circles) for BD-8 re-injection

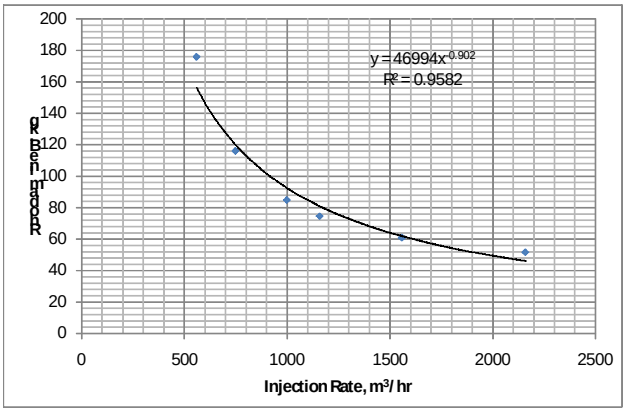

Figure 3: Injection rate tracer amount sensitivity plot

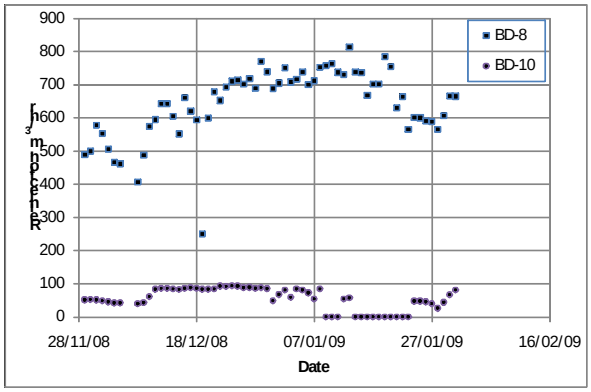

Figure 4: Injection rate changes during the tracer test

3. IMPLEMENTATION OF TRACER TEST

The flow rate, temperature and pressure measurements were conducted continuously in production and re-injection wells. Flow rates were measured using magnetic flow meters. Temperatures were measured using analogue and/or digital thermometers where appropriate. Pressures were recorded using pressure transmitters. Wellheads of reinjection wells BD-8 and BD-10 were modified for tracer test. All production well heads were prepared for sample collection purposes. A portable separator – condenser unit was used to collect samples. First NaCl salt was mixed thoroughly with geothermal water in a large tank with 1 tonne capacity and injected in BD-10 in less than an hour. Following that approximately 100 kg of Rhodamine B tracer was mixed with 1 tonne geothermal water and then injected as a slug into BD-8 well in approximately 2 hours. Prior to the tracer test calibration (baseline) samples were collected from each well. After that samples were collected in 1 litre sample bottles using the aforementioned separator – condenser unit. The *Rhodamine B* concentration was detected by using Turner Quantech Fluorimeter. Samples were placed in 3.5 ml Suprasil quartz cuvettes and 540 nm narrow band excitation and sharp cut 585 nm emission filters were used in measurements. First a calibration fluid is prepared for different concentrations (i.e. 0.1, 0.2, 0.4, 0.8, 1, 2, 4 and 8 ppb). Following that a calibration run is conducted. A regression constant, larger than 0.9, was used in all measurements. Following that samples were placed in round 3.5 ml cuvettes and measurements were conducted. Calibration was repeated each day as the *Rhodamine B* required re-calibration once the device is turned off. A similar procedure was followed to measure NaCl concentration using a chlorine electrode.

4. TRACER ANALYSIS

The flow of tracer between an injection and a production well pair has been described both analytically and numerically by number of authors. In this study, six different models were considered: multi-fracture model (Fossum and Horne, 1982), fracture-matrix model (Bullivant and O'Sullivan, 1989), uniform porous model (Sauty, 1980), double-porosity slabs model, double-porosity cubes model, and double-porosity pseudo-steady-state model (Bullivant and O'Sullivan, 1989). In each model it is assumed that there is a good connection between the injection and production wells along a streamline which is surrounded by a stream tube of constant cross section. The tracer is injected as a slug from the injection well and the response is recorded in the observation well. The models were matched to field data using non-linear-least-squares approximation using Microsoft's Excel. By minimizing the objective function *R* given in Equation 3, the parameters of the proposed analytical transfer functions can be estimated.

$$R = \sum_{i=1}^{n} w_i (C_{\mathrm{mod}\,el} - C_{field})^2 \qquad (3)$$

Here w_i's are the inverses of the variances of the experimental measurement errors, which will give the maximum-likelihood/minimum-variance estimates of the parameters. Model concentrations whose details are described elsewhere (Akin, 2001) can be obtained using the Equations 4 - 9.

1 D Homogeneous:

$$C_r = \frac{K}{t_r} Exp(-\frac{P_e}{4t_r}(1-t_r)^2) \qquad (4)$$

Single and Multi Fracture:

$$C_r = \frac{1}{2\sqrt{\frac{t_r}{P_e}}} Exp \frac{-(1-t_r)^2}{\frac{4}{P_e} t_r} \quad (5)$$

Fracture – Matrix:

$$C_r = JU(t-t_b)^{-1/2} Exp \frac{-t_b}{w(t-t_b)} \quad (6)$$

Double Porosity Pseudo Steady State:

$$C_r = JExp(-\alpha_m t)U(t-t_b)^{1/2} I_1(2(t_b \alpha_f \alpha_m (t-t_b))^{1/2}) \quad (7)$$

Double Porosity Slabs:

$$C_r = JExp(-t_b(2\sqrt{\frac{p}{wt_b}} \tanh(\frac{t_f}{2}\sqrt{\frac{p}{wt_b}}) + p)) \quad (8)$$

Double Porosity Cubes:

$$C_r = JExp(-t_b(2\sqrt{\frac{p}{wt_b}} \coth(\frac{t_f}{2}\sqrt{\frac{p}{wt_b}}) - \frac{4}{t_f} + p)) \quad (9)$$

In these equations P_e is Peclet number, w is ratio of transport along the fracture to transport out of the fracture, t_r is the tracer residence time, t_f is the matrix block fill up time, t_b is the time at which the pulse would reach the observation well if there was no dispersion or response start time, U is Heaviside step distribution, I_1 is the modifed Bessel function of the first kind of order 1; α_f is the rate of tracer interchange per unit fracture volume and α_m is the rate of tracer interchange per unit matrix volume, J is model parameter, and p is Laplace transform parameter.

Apart from the mathematical model exercises, a moment analysis method (Shook, 2003) that transforms tracer effluent data into Flow Capacity – Storage Capacity (*F*-*C*) diagrams was used to analyze the tracer effluent data. In this method the incremental flow capacity (f_i) of the i^{th} fracture, assuming injection and production pressures and fluid viscosity are equal, is the ratio of that fracture's flow capacity, k_iA_i/L_i, to the total network's flow capacity.

$$f_i = \frac{k_i A_i / L_i}{\sum_{j=1}^{N} k_j A_j / L_j} \quad (10)$$

Similarly, the fractional storage of the i^{th} fracture, is the pore volume of that fracture divided by the total fracture pore volume.

$$c_i = \frac{V_{pi}}{\sum_{j=1}^{N} V_{pj}} \quad (11)$$

The flow capacity, F, and storage capacity, C, are simple summations of the individual fracture f_i and c_i.

$$F_i = F_{i-1} + f_i \quad (12)$$

$$C_i = C_{i-1} + c_i \quad (13)$$

The derivative of F with respect to C is a ratio of the mean residence time divided by the residence time of the i^{th} fracture. If we assume equal length flow paths as we have done in our conceptual mathematical models, this ratio becomes a ratio of the interstitial velocity of the i^{th} fracture normalized by the mean velocity of the network. Thus the number of fractures and their fractional pore volume are identified from the inflection points on interstitial velocity curve (Wu et al, 2008).

5. RESULTS AND DISCUSSIONS

In all of the production wells Rhodamine B breakthrough and an increase in NaCl concentration has been observed. Peak Rhodamine B concentrations and corresponding breakthrough times differed from well to well. The highest and lowest peak Rhodamine B concentrations were observed in BD-5 and BD-3 respectively. On the other hand, highest and lowest peak NaCl concentrations were observed in BD-12 and B-10 or BD-14. Figures 5 and 6 show the direction of flow of Rhodamine B and NaCl formed using the information provided in Table 2. In these plots red arrows show the fastest flow followed by slower yellow and slowest blue arrows. These flow directions suggest that flow is mainly along the high conductivity Agamemnon fault. High concentrations of tracer and breakthrough data observed in wells like BD-5 suggest that tracer leaves the high conductivity channel and enters several fracture networks that are aligned orthogonal to Agamemnon fault. It was observed that NaCl flow directions are somewhat slower than the ones observed for Rhodamine B. This was expected due to the injection rate differences between BD-8 and BD-10. As the average injection rate in BD-10 is an order of magnitude smaller than that of BD-8 NaCl tracer finds more time to enter these fracture networks. These findings are confirmed with mathematical modeling results. In all Rhodamine B tracer return curves dispersion was somewhat smaller compared to ones obtained for NaCl (Figures 7 through 10). Generally, double porosity models (i.e. slabs, cubes or pseudo steady state) represented NaCl tracer return curves better than the other models with a few exceptions (BD-12 and BD-14) where fracture-matrix model performed better. In double porosity cubes model the rock matrix consists of cubic blocks of side *b* separated by high permeability fractures of aperture *a*. The double-porosity cubes model differs from the double- porosity slabs model because for the cubes model, the area of the surface at distance b/2+z from the nearest fracture is proportional to the square of z, whereas for the slabs model the area of the surface at distance b/2+z from the nearest fracture does not vary with z. This affects the way tracer diffuses into the block. Tracer movement in the blocks is modeled by diffusion perpendicular to the nearest face. In these models the reservoir contains uniformly distributed high-permeability micro fractures which divide the reservoir into low-permeability blocks that consist of pores unswept by the fluid flow. Similar to the mechanism defined for the fracture-matrix model, the tracer leaves the micro-fractures and then returns again. However, the effect is different, such that the blocks may be filled with tracer. The Peclet numbers were <1, that corresponded to a diffusion-dominated system unlike the multi-fracture model's (BD-12

and BD-14) convection-dominant system. For the shallow wells the fracture/matrix porosity ratio was found to be changing between 0.002 and 0.004. Satman et al (2002) reported that shallow wells' (such as B-2, B-3 and B-5) porosity values changed between 2% to 5%. Using these values, it can be found that porosity of the fractures change between $4x10^{-3}$% and 0.02%. Rhodamine B tracer matches showed that rather than double porosity models fast tracer returns can be modeled by fracture matrix and multifracture models. This suggests that tracer particles do not find time to leave the high conductivity channel and enter several fracture networks that are aligned orthogonal to Agamemnon fault. That's why it is believed that the tracer leaves the micro-fractures and then returns again. In several cases (i.e. BD-2, BD-9 and BD-11) although the tracer was detected it was not possible to analyze the return curves due to noisy nature of the data. Yet another important observation was that even though the test was designed to detect a peak concentration of 10 ppb in each well this value was never reached.

Table 2. Rhodamine B and NaCl mean arrival times, peak and baseline tracer concentrations observed during the tracer test and the models matched to these tests.

	Rhodamine Breakthrough time, (min)	NaCl Breakthrough time, (min)	Peak Rhodamine (ppb)	Peak NaCl (ppm)	Background NaCl (ppm)	Model (NaCl)	Model (Rhodamine)
B-10	1127.05	108.54	1.28	346	325	DP Cubes	FractureMatrix
BD-4	845.32	431.07	1.44	370	323	DP PSS	MultiFracture
BD-1	848.47	301.88	0.08	354	311	DP PSS	DP Slabs
B-5	850.11	380.33	0.38	336	320	DP Slabs	FractureMatrix
B-7	752.06	469.67	0.28	346	248	DP Slabs	FractureMatrix
BD-11	592.34	1815.12	0.05	370	346	DP Cubes	NA
BD-3	191.54	1037.04	2.37	390	346	DP Slabs	MultiFracture
BD-9	308.73	1532.55	0.38	377	317	DP Slabs	NA
BD-12	1025	2235.43	0.28	515	385	MultiFracture	DP Slabs
BD-15	1130.83	161.3	0.19	371	310	DP Cubes	MultiFracture
BD-7	1005.48	316.48	0.17	375	295	DP PSS	DP Slabs
BD-5	1335.72	521.74	2.48	374	316	DP Slabs	FractureMatrix
BD-2	428.03	812.07	0.32	433	343	DP Slabs	NA
BD-14	473.6	756.28	0.46	350	329	MultiFracture	NA
BD-6	654.36	620.2	2.35	370	331	DP Cubes	NA

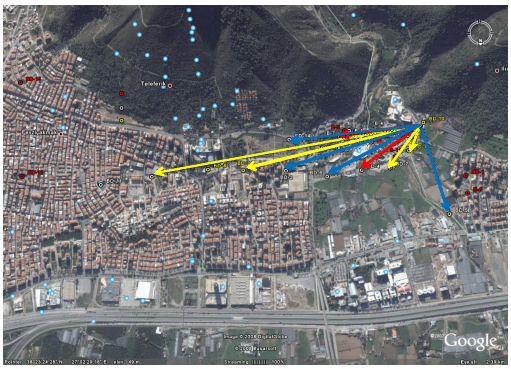

Figure 5: NaCl flow direction based on mean arrival times in production wells

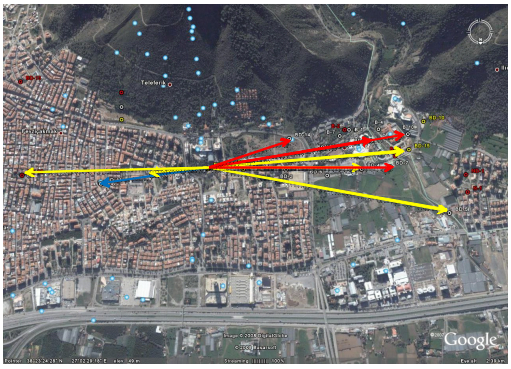

Figure 6: Rhodamine B flow direction based on mean arrival times in production wells

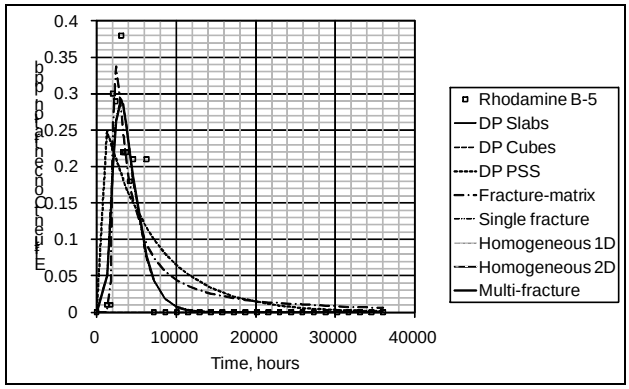

Figure 7. Rhodamine B return matches obtained for B-5

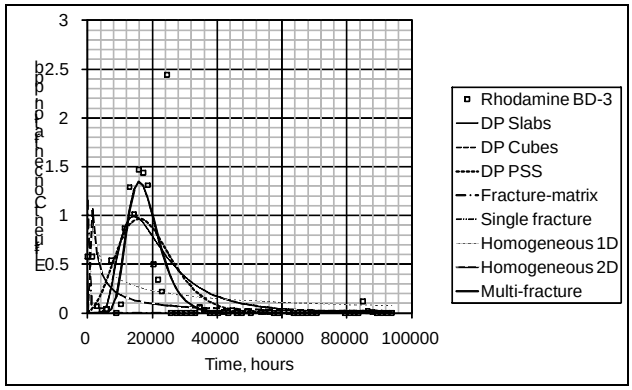

Figure 8. Rhodamine B return matches obtained for BD-1

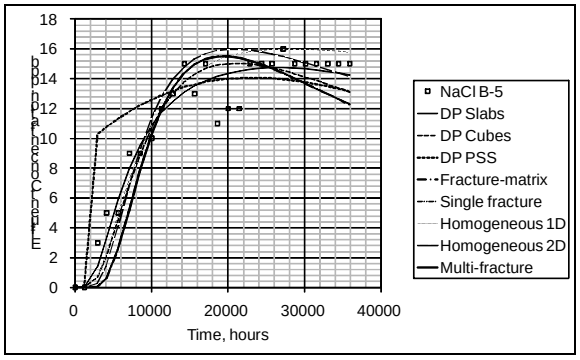

Figure 9. NaCl return matches obtained for B-5

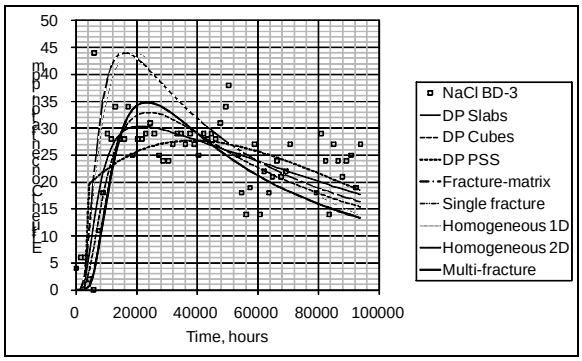

Figure 10. NaCl return matches obtained for BD-1

Using the aforementioned moment analysis method the tracer curves were analyzed. Figure 11 and 12 show a sample flow-storage capacity and interstitial velocity – storage capacity plots. Figure 11 tells us that 30% of flow comes from 20% of the fracture system near BD-6. Since the curve is somewhat close to 45° line (homogeneous fractures) the reservoir fracture system is not very heterogeneous around BD-6. The inflection points in Figure 12 tell us that there are few main flow paths (i.e. fractures) around the vicinity of BD-6. For these fractures the interstitial velocity is 1.2 times faster than the average velocity. Similar results were obtained for other wells. It was observed that as the production well gets deeper the number of interstitial velocity inflection points becomes abundant apart from a few exceptions such as B-10's behavior (Figure 13). It can be seen that the inflection points are as many as that of BD-6's. However, the average velocity of such fractures is more compared that of BD-6's.

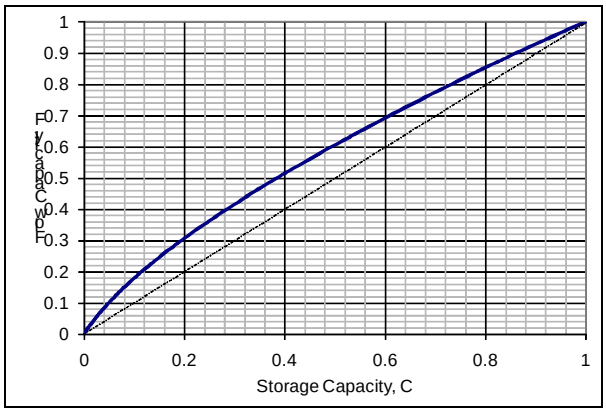

Figure 11. Flow – storage capacity plot of BD-6 derived from NaCl tracer return data

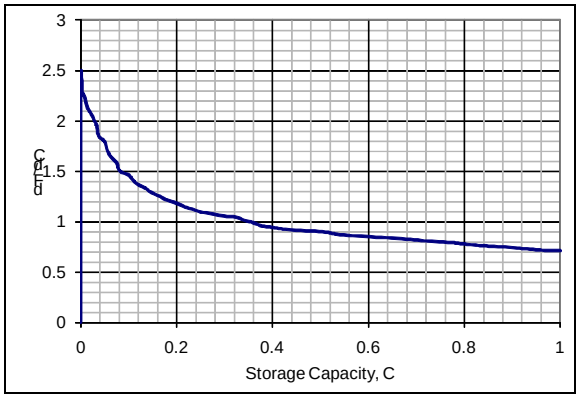

Figure 12. Derivative flow (interstitial velocity) – storage capacity plot of BD-6 derived from NaCl tracer return data

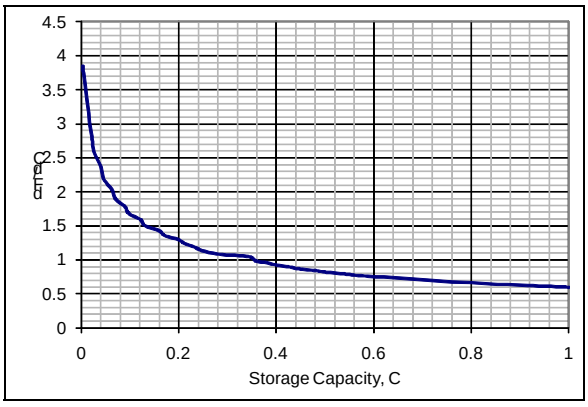

Figure 13. Derivative flow (interstitial velocity) – storage capacity plot of B-10 derived from NaCl tracer return data

CONCLUSIONS

A successful two well tracer test where Rhodamine B and NaCl salt has been injected from two separate injection wells in Balcova - Narlidere Geothermal field is reported. The tracer test that has been designed using EHDT method was analyzed using several analytical models and moment analysis technique. Since Rhodamine B was observed and the NaCl concentration increased in all wells it was concluded that the production and injection wells are connected along the Agamemnon fault. Presence of several orthogonal fracture systems was shown by mean arrival time arrow plots. Mathematical modeling results showed that NaCl tracer profiles were modeled by double porosity models. On the other hand, Rhodamine B tracer return curves were matched with fracture-matrix and multifracture models. Using moment analysis of the NaCl tracer return data the heterogeneity around the vicinity of production wells were identified. It was found that as the production well depth becomes deeper the number of interstitial velocity inflection points increases showing that the well produces from more than one fracture systems.

ACKNOWLEDGEMENTS

We would like to thank to Izmir Geothermal Energy Co. for allowing us to present this paper.

REFERENCES

Akin, S. (2001) "Analysis of Tracer Tests with Simple Spreadsheet Models" Computers & Geosciences, 27, 2, 171-178.

Aksoy, N., 2001. Monitoring the Balcova–Narlidere geothermal system using tracers. Ph.D. Dissertation, Dokuz Eylul University Graduate School, Izmir, Turkey, 150 pp. (in Turkish).

Aksoy, N., Serpen, U., Filiz, S., 2008. Management of the Balcova–Narlidere geothermal reservoir, Turkey. Geothermics.

Ercan, A., Drahor, M., Atasoy, E., 1986. Natural polarization studies at Balcova geothermal field. Geophys. Prospect. 34, 475–491.

Field M. S. (2003). "A review of some tracer-test design equations for tracer-mass estimation and sample-collection frequency." Environ Geol 43 (8): 867-881.

Satman, A., Serpen, U. Onur, M. 2002 izmir balçova-narlidere jeotermal sahasinin rezervuar ve üretim performansi projesi. Report prepared for Balcova Jeothermal (In Turkish).

Shook M. G. 2003. A Simple, Fast Method of Estimating Fractured Reservoir Geometry from Tracer Tests. Trans., Geothermal Resources Council, Vol. 27, 2003.

Tezcan, K., 1962. Izmir (Agamemnon) Resistivity survey. General Directorate of Mineral Research and Exploration (MTA) Report #3214. Ankara, Turkey, 80 pp. (In Turkish).

Wu, X., Pope, G.A., Shook, M.G., Srinivasan,S. 2008. Prediction of enthalpy production from fractured geothermal reservoirs using partitioning tracers. Int J Heat & Mass Trans, vol 51, 5-6, 1453-1466.